WATER RESOURCES RESEARCH, VOL. 49, 8174–8186, doi:10.1002/2012WR012795, 2013

Evaluation of the successive V6 and V7 TRMM multisatellite precipitation analysis over the Continental United States

Sheng Chen,[1,2] Yang Hong,[1,2] Jonathan J. Gourley,[3] George J. Huffman,[4,5] Yudong Tian,[5,6] Qing Cao,[1,2] Bin Yong,[7] Pierre-Emmanuel Kirstetter,[1,2,3] Junjun Hu,[2,8] Jill Hardy,[2,3] Zhe Li,[9] Sadiq I. Khan,[1,2] and Xianwu Xue[1,2]

Received 14 August 2012; revised 25 July 2013; accepted 17 October 2013; published 10 December 2013.

[1] The spatial error structure of surface precipitation derived from successive versions of the TRMM Multisatellite Precipitation Analysis (TMPA) algorithms are systematically studied through comparison with the Climate Prediction Center Unified Gauge daily precipitation Analysis (CPCUGA) over the Continental United States (CONUS) for 3 years from June 2008 to May 2011. The TMPA products include the version-6(V6) and version-7(V7) real-time products 3B42RT (3B42RTV6 and 3B42RTV7) and research products 3B42 (3B42V6 and 3B42V7). The evaluation shows that 3B42V7 improves upon 3B42V6 over the CONUS regarding 3 year mean daily precipitation: the correlation coefficient (CC) increases from 0.85 in 3B42V6 to 0.92 in 3B42V7; the relative bias (RB) decreases from −22.95% in 3B42V6 to −2.37% in 3B42V7; and the root mean square error (RMSE) decreases from 0.80 in 3B42V6 to 0.48 mm in 3B42V7. Distinct improvement is notable in the mountainous West especially along the coastal northwest mountainous areas, whereas 3B42V6 (also 3B42RTV6 and 3B42RTV7) largely underestimates: the CC increases from 0.86 in 3B42V6 to 0.89 in 3B42V7, and the RB decreases from −44.17% in 3B42V6 to −25.88% in 3B42V7. Over the CONUS, 3B42RTV7 gained a little improvement over 3B42RTV6 as RB varies from −4.06% in 3B42RTV6 to 0.22% in 3B42RTV7. But there is more overestimation with the RB increasing from 8.18% to 14.92% (0.16–3.22%) over the central US (eastern).

Citation: Chen, S., et al. (2013), Evaluation of the successive V6 and V7 TRMM multisatellite precipitation analysis over the Continental United States, *Water Resour. Res.*, *49*, 8174–8186, doi:10.1002/2012WR012795.

1. Introduction

[2] Reliable quantitative estimates of the spatial precipitation distribution play a critical role in the application of satellite-based precipitation in hydrologic modeling and hazards monitoring and forecasting. Satellite-based quantitative precipitation estimates (QPE) products are widely used for such applications due to their global coverage and spatial continuity. However, the inherent error sources in satellite-based measurements (e.g., the spatiotemporal variation of the precipitation fields and the system errors in the instruments) have not yet been well understood. Therefore, characterizing the error structure of satellite-based precipitation products is recognized as a major issue for the usefulness of the estimates [*Hong et al*., 2006]. Additionally, a quantification of the error characteristics is necessary for data assimilation, climate analysis [*Stephens and Kummerow*, 2007], and hydrological modeling of natural hazards [*Hong and Adler*, 2007].

[3] To define these spatial error characteristics, the TRMM Multisatellite Precipitation Analysis (TMPA) algorithm, developed by the National Aeronautics and Space Administration (NASA) Goddard Space Flight Center (GSFC) [*Huffman et al*., 2007], was used. The TMPA provides a 3 h, real-time, gridded precipitation product (3B42RT, hereafter 3B42RTV6 for Version-6 and 3B42RTV7 for Version-7) with a coverage area of 60°N–60°S and a gauge-adjusted, post-real-time research version product (3B42) with a spatial resolution of 0.25° × 0.25° within the global latitude belt 50°N–50°S. Version-6 3B42 (hereafter, 3B42V6) has seen wide applications in

[1]School of Civil Engineering and Environmental Science, University of Oklahoma, Norman, Oklahoma, USA.
[2]Advanced Radar Research Center, National Weather Center, Norman, Oklahoma, USA.
[3]NOAA/National Severe Storms Laboratory, Norman, Oklahoma, USA.
[4]Science Systems and Applications, Inc., Lanham, Maryland, USA.
[5]NASA Goddard Space Flight Center, Greenbelt, Maryland, USA.
[6]Earth System Science Interdisciplinary Center, University of Maryland, College Park, Maryland, USA.
[7]State Key laboratory of Hydrology-Water Resources and Hydraulic Engineering, Hohai University, Nanjing, China.
[8]School of Computer Science, University of Oklahoma, Norman, Oklahoma, USA.
[9]Departments of Hydraulic Engineering, Tsinghua University, Beijing, China.

Corresponding author: Y. Hong, School of Civil Engineering and Environmental Science, University of Oklahoma, 202 W. Boyd St., Norman, OK 73072, USA. (yanghong@ou.edu)

0043-1397/13/10.1002/2012WR012795

hydrologic communities [*Su et al*., 2008; *Wu et al*., 2012; *Yong et al*., 2010], but the algorithm was no longer yielding outputs as of 30 June 2011. Version-7 3B42 (hereafter, 3B42V7) is the latest version of a gauge-adjusted, post-real-time TRMM product, which became available for the time period of 1998–present in late May 2012, and supersedes all previous versions. Many studies have been carried out to validate 3B42RTV6 and 3B42V6 and have revealed their systematic and random errors[*Chen et al*., 2009; *Gourley et al*., 2010; *Shen et al*., 2010; *Stampoulis and Anagnostou*, 2012; *Tian et al*., 2010; *Zhou et al*., 2008]. However, few of them reveal the spatial error over a large scale, such as the CONUS or the globe. Furthermore, the newly available 3B42RTV7 and 3B42V7 requires similar validation and more importantly, comparison to the previous version TMPA since V7 presumably would be a better algorithm. Furthermore, it could evolve into the initial Version-0 product for the upcoming Global Precipitation Measurement (GPM) mission to be launched in 2014. The objectives of this paper are to study the multiannual and seasonal spatial error structure of V7 TMPA over the CONUS relative to V6 and to enable the algorithm developers to further improve the precipitation retrieval algorithms in anticipation of GPM.

2. Data and Methods

[4] The original intent of this study was to evaluate the 3 hourly TMPA products using the hourly Stage IV rainfall product as reference. However, the hourly Stage IV are not available in the northwest US due to the River Forecast Center (RFC) not using the same protocols in terms of generating Stage IV precipitation products at hourly resolution [*Chen et al*., 2013]. Additionally, the hourly Stage IV data apply the Parameter-elevation Regressions on Independent Slopes Model (PRISMs)-based climatologies developed by *Daly et al*. [1994] in their spatial interpolation of gauge data over the West. In these regions, the Stage IV precipitation product does not use weather radar to depict spatial precipitation patterns, but rather relies on the monthly climatological patterns. Therefore, the newly available gridded analysis of the gauge data set produced by the National Oceanic and Atmospheric Administration (NOAA) Climate Prediction Center (CPC) is selected as the ground reference data, and referred to as the CPC Unified Gauge daily precipitation Analysis (CPCUGA) [*Chen et al*., 2008b].An optimal interpolation (OI) technique was employed in the CPCUGA to project gauge reports over the CONUS to a 0.25° grid based on PRISMs. The OI was used because it has been shown to have higher correlation with individual gauge measurements than other techniques [*Chen et al*., 2008b]. The gauge reports are derived from three sources: NOAA's National Climate Data Center (NCDC) daily co-op stations, CPC data set (River Forecast Centers data + 1st order stations), and daily accumulations from hourly precipitation data set (1948-...). Duplicates and overlapping stations were removed during data QC control, and standard deviation and buddy checks were applied. According to an early study by *Chen et al*. [2008], the CPCUGA has a bias of −0.467% and a correlation with gauge observations of about 0.811 from 1979 to 2008 [*Chen et al*., 2008a]. More details can be seen on the official website: http://www.esrl.noaa.gov/psd/data/gridded/data.unified.daily.conus.html.

[5] 3B42RTV6 and 3B42RTV7 are nearly real-time products computed with the TMPA algorithm, while 3B42V6 and 3B42V7 are post-real-time products computed with the Version-6 and Version-7 TMPA algorithms. Sources of passive microwave satellite precipitation estimates include TRMM Microwave Imager (TMI), Special Sensor Microwave Imager (SSMI), Special Sensor Microwave Imager/Sounder (SSMIS) (3B42V7 only), Advanced Microwave Scanning Radiometer-EOS (AMSR-E), Advanced Microwave Sounding Unit-B (AMSU-B), and Microwave Humidity Sounder (MHS). Also, during the period of 1998–1999, the 3B42V7 includes the 0.07° Grisat-B1 infrared data, which represents a significant improvement in resolution and areal coverage over the 1° 24 class histogram infrared data used in Version-6. Finally, the 3B42V7 incorporates the new Global Precipitation Climatology Centre (GPCC) "full" gauge analysis whenever available, and the GPCC "monitoring" gauge analysis since 2010; whereas, the previous monitoring product encompassed periods up to April 2005 and used the Climate Assessment and Monitoring System (CAMS) analysis thereafter [*Huffman et al*., 2011]. The major changes from V6 to V7 are mainly from three factors: (1) the enhanced TMPA Level-2 products, (2) use of the GPCC data with improved climatology and anomaly analysis, and (3) more satellite observations incorporated. Based on previous studies on the level-2 product evaluation of successive V6 and V7 TRMM PR (i.e., 2A25 or PRV7) done by *Chen et al*. [2012a] and *Kirstetter et al*. [2013], the PRV7 gained small to moderate improvement over PRV6 with relative difference (bias) decreasing from −22.09% to −18.38%, RMSE decreasing from 7.47 mm to 7.18 mm. For the gauge input sources, both V6 and V7 use two different sources of gauge analyses: (1) CAMS for initial processing and (2) previous GPCC monitoring gauge analysis for retrospective processing. However, the gauge products used in V7 shifted to an improved climatology and anomaly analysis, including improvements in complex terrain [*Huffman et al*., 2011]. In addition, V7 blends more satellite observation data, including SSMIS and 0.07° Grisat-B1 infrared data, which represents an improvement in resolution and areal coverage over the 1° 24 class histogram infrared data used in Version-6. More details can be seen in *Huffman and Bolvin* [2013] and *Huffman et al*. [2011].

[6] Since the CPCUGA is a daily product with the same spatial resolution as TMPA products, we accumulated the 3 h precipitation estimates of TMPA products to daily precipitation estimates. The data range were chosen to be 3 years from June 2008 to May 2011, about 1 month before the end of the production of 3B42V6. The readers should bear in mind that the gauges used in CPCUGA might not be completely independent from GPCC used for bias-correction in TMPA research version data. However, over the CONUS, GPCC only contains a small subset of the gauges collected by CPCUGA, a maximum of 570 out of 2492 gauges potentially used in both data sets. In addition, GPCC is only used at a monthly, 1° scale for TMPA bias correction. Granted TMPA's bias performances at this scale or coarser will benefit from GPCC. But at daily, 0.25° scale, TMPA's information content is still massively dominated by satellite

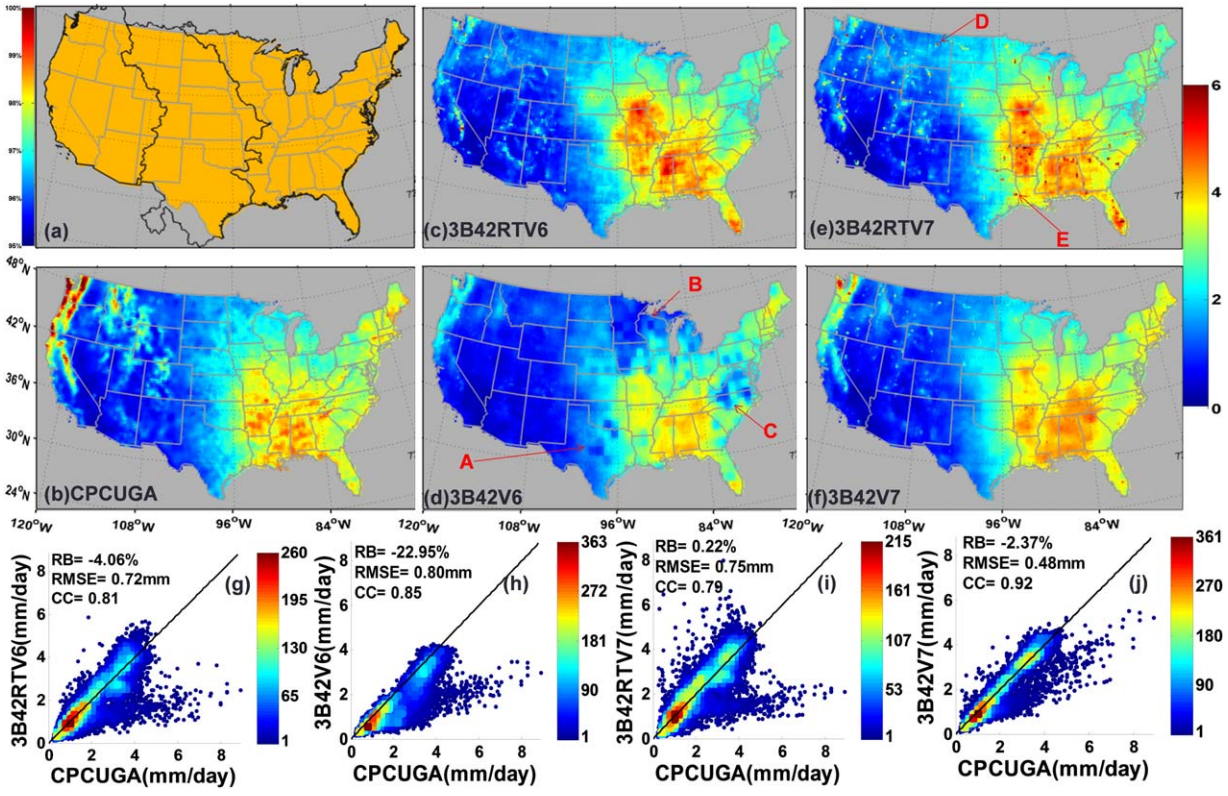

Figure 1. (a) Data availability, (b–f) 3 year mean daily rainfall of V6/V7 TMPA over CONUS, and (g–j) density-color scatter plots of TMPA versus CPCUGA. The solid dark lines in Figure 1a outline the boundaries of the West, Central and East CONUS.

sensors since the GPCC only provides an overall bias adjustment ratio that is spatiotemporally varying, but only uniformly applied to the entire month. For more explanation, please refer to previous study in *Bolvin et al*. [2009]. Therefore, it is reasonable to compare TMPA and CPCUGA when one is looking at high-resolution error characteristics, which are not substantially affected by GPCC (personal communication with TMPA data developers Bolvin and Huffman). Bias (the difference between the TMPA and the reference), relative bias (RB, the Bias divided by the reference), root mean square error (RMSE), and the Pearson linear correlation coefficient (CC) are statistics used for the evaluation. RB, when multiplied by 100, denotes the degree of overestimation or underestimation in percent. All of the above statistics have been computed on a pixel-by-pixel basis over the CONUS.

3. Results and Discussion

3.1. Multiannual Precipitation

[7] Figure 1 shows the joint data availability of TMPA and CPCUGA and 3 year mean daily precipitation for each product as well as the corresponding density-colored scatterplots of the TMPA products versus CPCUGA data sets. The joint data availability reaches up to 98%. Generally, both versions of TMPA data sets captured the precipitation spatial patterns. However, differences are notable. The 3B42V6 captured the intense precipitation in the southeast CONUS, but failed to reveal precipitation maxima in the West, as well as in the states of Minnesota, Wisconsin, and Illinois. The areas indicated by the red letters A, B, and C in Figure 1d show rectangular-shaped underestimated areas, which indicate that the gauge-adjusted algorithm in V6 has problems in these areas. The 3B42RTV6 captured the intense precipitation in the central and southeast CONUS, but failed with the orographic precipitation on the west coast and in the New England states. The 3B42RTV7 shows close spatial patterns with 3B42RTV6 with a little less intense precipitation than 3B42RTV6 in the central and southern CONUS. Note that 3B42RTV7 reveals very high maxima at individual pixels, especially in the mountainous West and the southern CONUS (e.g., the pixels indicated by red letters D and E in Figure 1e). Spatial patterns of 3 year mean daily precipitation depicted by 3B42V7, on the other hand, agree quite well with the reference CPCUGA. The most notable improvements are in the northeast CONUS and northwest CONUS where there is orographic precipitation on the west coast. In addition to the slight improvements of the TMPA Level-2 retrieval algorithm[*Chen et al*., 2012a; *Kirstetter et al*., 2013], this is likely due to more gauge observations and improved climatology/anomaly analysis used in 3B42V7. Figures 1g–1j show density-colored scatterplots of the TMPA products versus CPCUGA data sets for 3 year mean daily precipitation. Table 1 summarizes their corresponding statistics for the west, central, and east CONUS. These scatterplots illustrate that 3B42V7 performed better in quantifying precipitation amounts than the other three products in terms of

RB, RMSE, and CC. It has the highest CC with 0.92 and a small bias with −2.37%. Moreover, its RMSE is much lower than those with the other products. The 3B42V6 product severely underestimated the precipitation by a great margin of 22.95% with a little lower CC of 0.85, higher RMSE of 0.80 when compared to 3B42V7. Some of the deficiencies in 3B42V6 very likely originated from the gauge data used, as evidenced by the low values in the areas denoted by the red letters in Figure 1d. The 3B42RTV6 and 3B42RTV7 products have similar skill scores with RB of −4.06% and 0.22%; RMSE of 0.72 and 0.75; and CC of 0.81 and 0.79, respectively. The 3B42RTV7 gains a little improvement over 3B42RTV6 over the CONUS in terms of bias.

[8] Table 1 indicates that 3B42V7 improves noticeably along the coastal mountainous areas in the northwest CONUS, whereas 3B42V6 largely underestimated; the CC increases from 0.86 in 3B42V6 to 0.89 in 3B42V7; and the RB decreases from −44.17% in 3B42V6 to −25.88% in 3B42V7. Besides, impressive improvement is also notable in the central and east CONUS with the RB decreasing from −15.06% in 3B42V6 to −0.07% in 3B42V7 in Central and from −19.20% in 3B42V6 to 4.91% in 3B42V7 in the East. The 3B42RTV7 product gained a marginal improvement over 3B42RTV6 as RB decreases from −31.94% to −27.97% over the West. But it has more overestimation with the RB increasing from 8.18% to 14.92% (0.16–3.22%) over the central US (East).

3.2. Seasonal Precipitation

[9] Precipitation varies spatially and temporally to a great extent over the CONUS. Figure 2 shows that the rainy seasons in the West are in winter and spring, but in the Central and East, rainy seasons are in spring and summer. Generally, 3B42V7 decently captured the precipitation pattern in every season and displayed spatially smooth and continuous variations of precipitation from the low to high precipitation areas. It is worth noting that only 3B42V7 captured the precipitation maxima on the western coastal mountainous belts in spring, autumn, and winter. The 3B42V6 product still shows the rectangular-shaped underestimated areas in every season, as shown in the 3 year mean daily precipitation (Figures 2i–2l and Figure 1d). The 3B42RTV6 and 3B42RTV7 show similar performance with close spatial precipitation patterns with CPCUGA. But both of these two products show overestimation in central-south CONUS in spring, summer, and winter. Additionally, all TMPA products failed to capture the precipitation maxima in the intermountain regions of the northwest CONUS (i.e., regions indicated by red letter A in Figure 2a) in spring, autumn, and winter (in particular). These intermountain regions were covered by snow and ice during these three seasons and are beyond the coverage (38°N-S) of TRMM. The high quality (HQ) algorithm, which derives the precipitation estimates from macrowave (MW) data in TMPA, has limitations in providing estimates in regions with frozen or icy surfaces [*Huffman and Bolvin*, 2013]. On the other hand, the IR-based variable rain rate product 3B41RT, which is used to fill the gaps wherever HQ is missing [*Huffman and Bolvin*, 2013], also has limitations in estimating rainfall in complex terrain [*Chen et al*., 2012b; *Hirpa et al*., 2010; *Negri and Adler*, 1993; *Tuttle et al*., 2008]. The central and southern CONUS are frequented by more convective and frontal events containing cold rain microphysics and ice in the spring and summer months, which apparently causes the overestimation of 3B42RTV6 and 3B42RTV7 here.

[10] Scatterplots in Figure 3 and Table 1 give the statistical scores regarding RB, RMSE, and CC for TMPA

Table 1. RB, RMSE, and CC for 3 Year and Four Seasonal Precipitations in Each Region

Indexes	Time	Type	CONUS	West	Central	East
RB (%)	3 Years	3B42RTV6	−4.06	−31.94	8.18	0.16
		3B42V6	−22.95	−44.17	−15.06	−19.20
		3B42RTV7	0.22	−27.97	14.92	3.22
		3B42V7	−2.37	−25.88	−0.07	4.91
	Spring	3B42RT V6	−22.62	−51.26	−22.66	−11.55
		3B42V6	−23.10	−43.31	−17.53	−18.04
		3B42RTV7	−14.93	−34.43	−10.17	−9.67
		3B42V7	−4.50	−28.77	−3.36	4.25
	Summer	3B42RT V6	15.49	29.23	28.37	6.05
		3B42V6	−17.37	−25.66	−10.37	−20.17
		3B42RTV7	16.63	3.13	25.65	13.65
		3B42V7	3.11	−5.80	3.47	4.32
	Autumn	3B42RT V6	−11.56	−28.23	5.25	−14.40
		3B42V6	−24.38	−42.31	−15.29	−23.09
		3B42RTV7	−2.55	−25.12	16.33	−4.71
		3B42V7	−1.50	−16.88	1.82	1.89
	Winter	3B42RT V6	2.68	−40.88	25.06	25.17
		3B42V6	−28.91	−52.83	−23.38	−14.74
		3B42RTV7	1.33	−35.85	38.76	15.03
		3B42V7	−8.03	−36.21	−7.24	10.35
RMSE	3 Years	3B42RT V6	0.72	1.06	0.46	0.55
		3B42V6	0.80	1.06	0.48	0.79
		3B42RTV7	0.75	1.10	0.53	0.58
		3B42V7	0.92	0.74	0.33	0.33
	Spring	3B42RT V6	1.08	1.52	0.80	0.87
		3B42V6	0.93	1.27	0.60	0.86
		3B42RTV7	1.01	1.49	0.61	0.84
		3B42V7	0.67	1.04	0.45	0.45
	Summer	3B42RT V6	1.01	0.50	1.25	1.04
		3B42V6	0.79	0.38	0.63	1.09
		3B42RTV7	0.98	0.63	1.10	1.07
		3B42V7	0.44	0.31	0.46	0.50
	Autumn	3B42RT V6	0.83	1.15	0.47	0.77
		3B42V6	0.86	1.03	0.49	0.90
		3B42RTV7	0.84	1.20	0.60	0.67
		3B42V7	0.46	0.61	0.35	0.40
	Winter	3B42RT V6	1.19	1.77	0.56	1.04
		3B42V6	1.07	1.81	0.47	0.59
		3B42RTV7	1.17	1.76	0.68	0.91
		3B42V7	0.81	1.33	0.41	0.47
CC	3 Years	3B42RT V6	0.81	0.66	0.88	0.72
		3B42V6	0.85	0.86	0.86	0.84
		3B42RTV7	0.79	0.54	0.87	0.68
		3B42V7	0.92	0.89	0.92	0.91
	Spring	3B42RT V6	0.80	0.64	0.84	0.83
		3B42V6	0.86	0.83	0.87	0.89
		3B42RTV7	0.78	0.52	0.87	0.79
		3B42V7	0.90	0.84	0.91	0.93
	Summer	3B42RT V6	0.87	0.78	0.86	0.74
		3B42V6	0.90	0.87	0.83	0.71
		3B42RTV7	0.90	0.61	0.85	0.77
		3B42V7 V6	0.96	0.86	0.91	0.88
	Autumn	3B42RT V6	0.79	0.66	0.90	0.69
		3B42V6	0.86	0.91	0.92	0.78
		3B42RTV7	0.78	0.55	0.89	0.71
		3B42V7	0.94	0.93	0.95	0.88
	Winter	3B42RT V6	0.62	0.63	0.59	0.69
		3B42V6	0.77	0.79	0.72	0.91
		3B42RTV7	0.61	0.61	0.56	0.67
		3B42V7	0.84	0.87	0.77	0.94

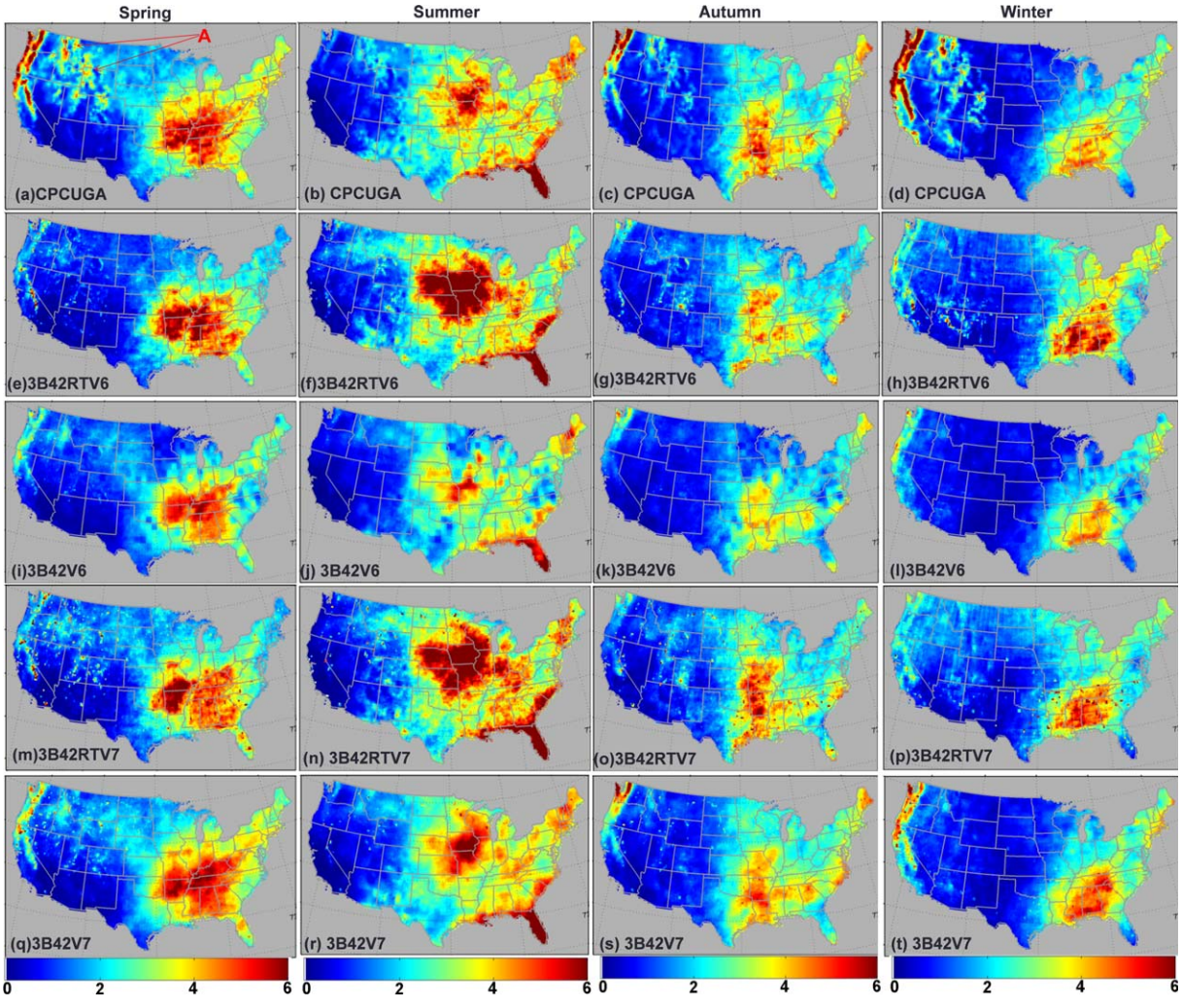

Figure 2. Seasonal mean daily precipitation over CONUS.

products during different seasons over the entire CONUS, West, Central, and East. The 3B42V7 product illustrates much better performance than the other three products from spring to winter. It has pretty high CCs of 0. 90, 0.96, 0.94, and 0.84 and marginal biases of −4.50%, 3.11%, −1.50%, and −8.03% over the CONUS for spring, summer, autumn, and winter, respectively. In contrast, 3B42V6 has lower CCs of 0.86, 0.90, 0.86, and 0.77 and more biased precipitation of −23.0%, −17.37%, −24.38%, and −28.91% over the CONUS for spring, summer, autumn, and winter, respectively. The 3B42V7 product also reduces the bias to a great extent during spring, autumn, and winter and decreases the overestimation by a great margin in summer over the West, Central, and East. Especially in the West, the underestimation decreases from −43.31% in 3B42V6 to −28.77% in 3B42V7 in spring, −25.66% in 3B42V6 to −5.80 in 3B42V7 in summer, −42.31% in 3B42V6 to −16.88% in 3B42V7 in autumn, and −52.83% in 3B42V6 to −36.21% in 3B42V7 in winter. During summer, the CC in the eastern CONUS increases from 0.71 in 3B42V6 to 0.88 in 3B42V7, while the RB decreased from −20.17% in 3B42V6 to 4.32% in 3B42V7, and the RMSE decreased from 1.09 mm in 3B42V6 to 0.50 mm in 3B42V7. More details can be seen in Table 1. The 3B42RTV7 shows a little better skill scores than 3B42RTV6 in spring and autumn and demonstrates similar scores in winter and summer. It reduced the underestimation from −22.62% (−11.56%) to −14.93% (−2.55%) in spring (autumn) over the entire CONUS. Over the West, the 3B42RTV7 decreased the underestimated precipitation from −51.26% (−40.88%) to −34.43% (−35.85%) in spring (winter). However, 3B42RTV7 overestimated the precipitation by 38.76% over the central CONUS during winter, much more than 3B42RTV6, which overestimated the precipitation by 25.06%.

3.3. Daily Series Statistics

[11] Daily precipitation is meaningful in hydrology and climatology; for example the three-layer Variable Infiltration Capacity (VIC-3L) hydrologic model [*Liang et al.*, 1996, 1994] is based on input of daily precipitation for hydrological and climatological applications. Figure 4 shows the variation of TMPA's area-average daily biased precipitation, CC and RMSE against CPCUGA over the CONUS and the three subregions. All TMPA data sets show an annual periodic variation with high scores of CC and RMSE during the warm season (April–September) and

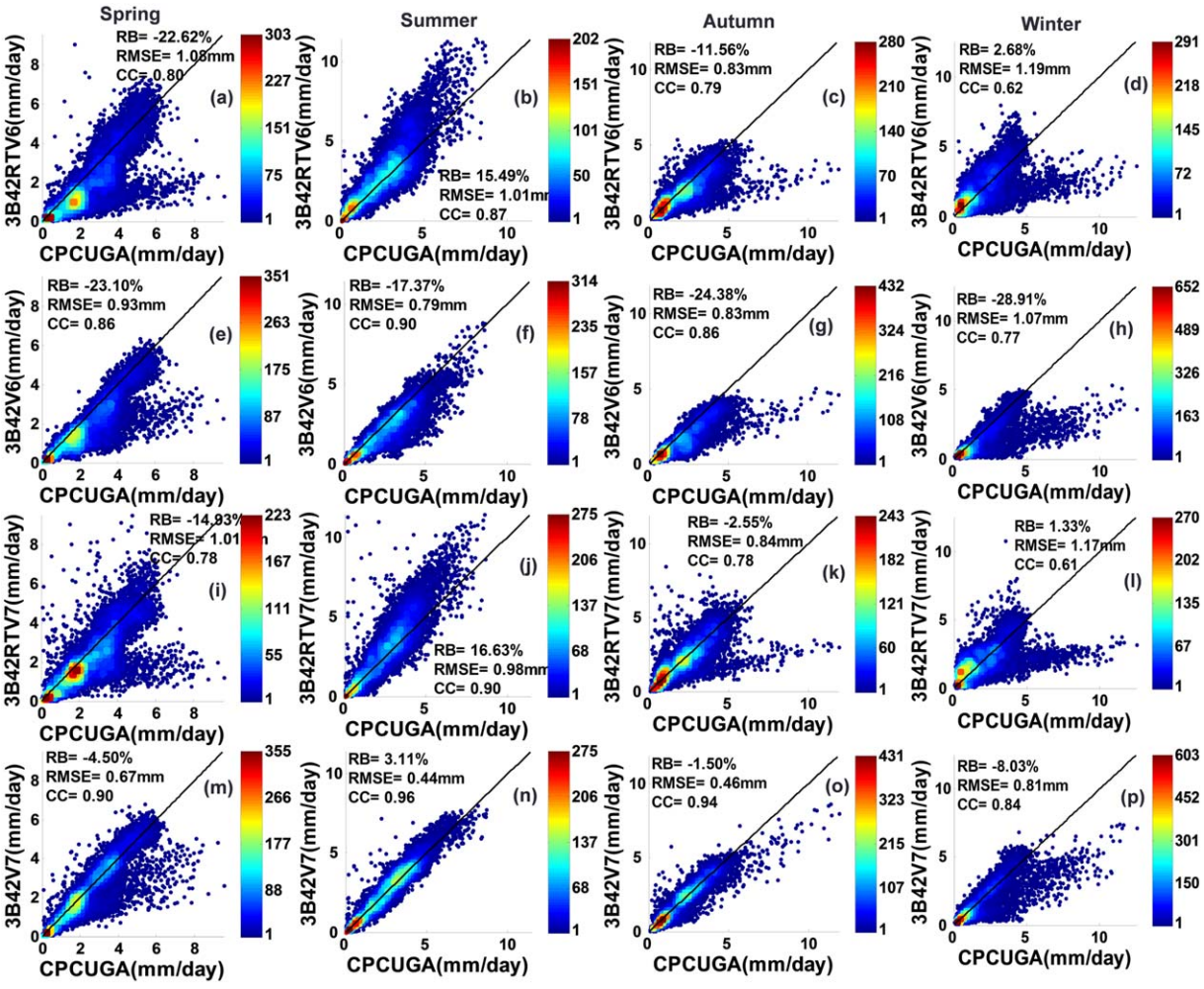

Figure 3. Scatterplots of TMPA versus CPCUGA for different seasonal mean daily precipitation over CONUS.

low scores in the cool season (October–March). However, this trend is not clearly seen for the daily bias. The daily bias values show much larger fluctuations. This result indicates that the TMPA products were greatly affected by the seasonal climate. The 3B42V7 demonstrates much lower bias in daily precipitation (−0.5 mm/day, 0.5 mm/day) and distinct higher daily series CC than the other three products over the CONUS (Figures 4a and 4b). The 3B42V6 product underestimated much of the precipitation over the CONUS all the time (Figure 4a). Prior to 2009, the 3B42RTV6 shows much overestimation and high RMSE in summer. However, the bias with 3B42RTV6 decreased dramatically, and RMSE with 3B42RTV6 decreased significantly in summer after 2009. This may be because of the calibrator of TMPA-V6 and the TRMM Combined Instrument (TCI) added to the V6 TMPA algorithm since October 2008[*Huffman et al*., 2010; *Yong et al*., 2012], and also added to the V7 TMPA algorithm. Compared to 3B42RTV6, the 3B42RTV7 shows more overestimation in summer but less underestimation in winter, higher daily CC and generally lower daily RMSE over the CONUS. It is worth noting that 3B42V6 underestimated rainfall in every region especially in the West and East. This indicates the algorithm of adjusting the 3B42RT product with the (GPCC) "full" gauge analysis applied in the V7 TMPA significantly improves the accuracy of precipitation estimates according to the CPCUGA product. The 3B42RTV7 product shows more pronounced overestimation than 3B42RTV6 during summer especially in the Central region. But in winter and spring, 3B42RTV6 demonstrates more overestimation than 3B42RTV7. In addition, the 3B42RTV6 shows much lower RMSE than 3B42RTV7. Generally, the post-research product 3B42 outperforms the real-time product 3B42RT in terms of Bias, CC, and RMSE; the 3B42V7 performs better than 3B42V6.

3.4. Probability Distributions by Occurrence and Precipitation Volume

[12] Probability distribution functions (PDFs) provide us with information on the precipitation rate distribution, precipitation volume distribution, and the precipitation estimates' sensitivity as a function of precipitation rate. This kind of evaluation also offers insight into error dependence on precipitation rate and the potential impact of the error on hydrological applications [*Tian et al*., 2010]. The PDFs by occurrence (PDFc) and by volume (PDFv) as a function of the daily precipitation are shown in Figures 5 and 6. Here, only grid cells where both the reference and the

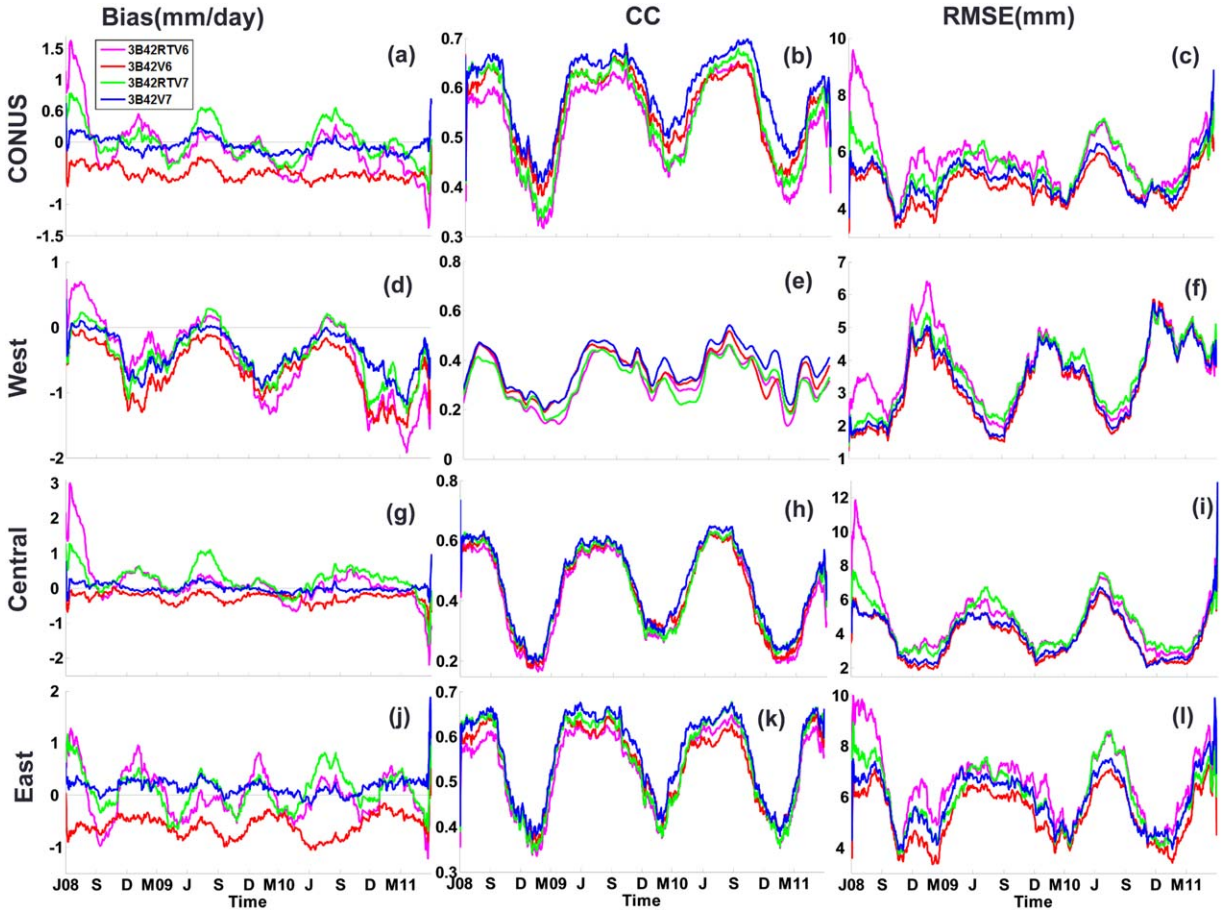

Figure 4. Daily bias, CC, and RMSE over CONUS, West, Central, and East.

TMPA precipitation estimates are nonzero can be selected to compute the PDFc and PDFv in order to emphasize the TMPA products' ability to quantitatively estimate precipitation when it is raining.

[13] As shown in Figures 6 and 7, the V6 and V7 TMPA products generally have similar distribution patterns of precipitation rates over CONUS and subregions both in occurrence and volume. The main differences of PDFc are clear at the lower end of bins (<4 mm/day) for PDFc and at bins of moderate rain rates (6–32 mm/day) for PDFv. All TMPA (especially V6) clearly overestimated the precipitation contributed by rain rates less than 6 mm/day and underestimated at rain rates 6–32 mm/day over the entire CONUS and all subregions for three years, winter and summer except the Central and East during the winter. In the central CONUS, all TMPA data sets except 3B42V6 overestimated the precipitation contributed by rain rates in the interval of 2–32 mm/day. In the East, the 3B42RTV6 overestimated the precipitation by a great deal for light rain rates (<6 mm/day) and underestimated precipitation contributed by rain rates in the 6–32 mm/day range. This is likely due to frozen precipitation (primarily snow) in the northeast CONUS in winter. HQ has limitations in providing estimates in regions with frozen or icy surfaces [*Huffman and Bolvin*, 2013]. The snow cover in winter very likely interferes with the PMW-based retrievals (i.e., HQ) [*Ferraro et al*., 1998; *Grody*, 1991], such as AMSR-E and AMSU-B with coverage of higher-latitude bands (beyond 38°N-S). The high frequency channels (89 and 150 GHz) of AMSU-B might detect more scattering associated with precipitation-sized ice particles in the winter atmosphere, which indirectly raises its retrieval precipitation rate [*Vila et al*., 2007; *Yong et al*., 2010]. In addition, the IR-based variable rainrate product 3B41RT, which is used to fill the gaps wherever HQ is missing [*Huffman and Bolvin*, 2013], has limitations in precipitation estimation [*Chen et al*., 2012b; *Hirpa et al*., 2010; *Negri and Adler*, 1993; *Tuttle et al*., 2008], especially for warm-top stratiform cloud systems during the cold season [*Tian et al*., 2007; *Vicente et al*., 1998]. What's more, the 3B42V6 suffered from systematical underestimation in the states of Minnesota, Wisconsin, and Illinois where are indicated by red letter A, B, and C in Figure 1d with rectangular-shaped underestimated areas. In the western CONUS, both 3B42RTV6 and 3B42V6 largely overdetected lighter precipitation rates (<4 mm/day), and underdetected precipitation rates higher than 4 mm/day, especially in winter. It should be noted that 3B42RTV7 overestimated the precipitation by a great margin in the rain rates from 2 to 16 mm/day especially in the West during winter time. This agrees with the rainfall intensity distribution for winter shown in Figure 2p. This may be because winter is the wet season in the West (particularly in the coastal areas; see Figure 2d).

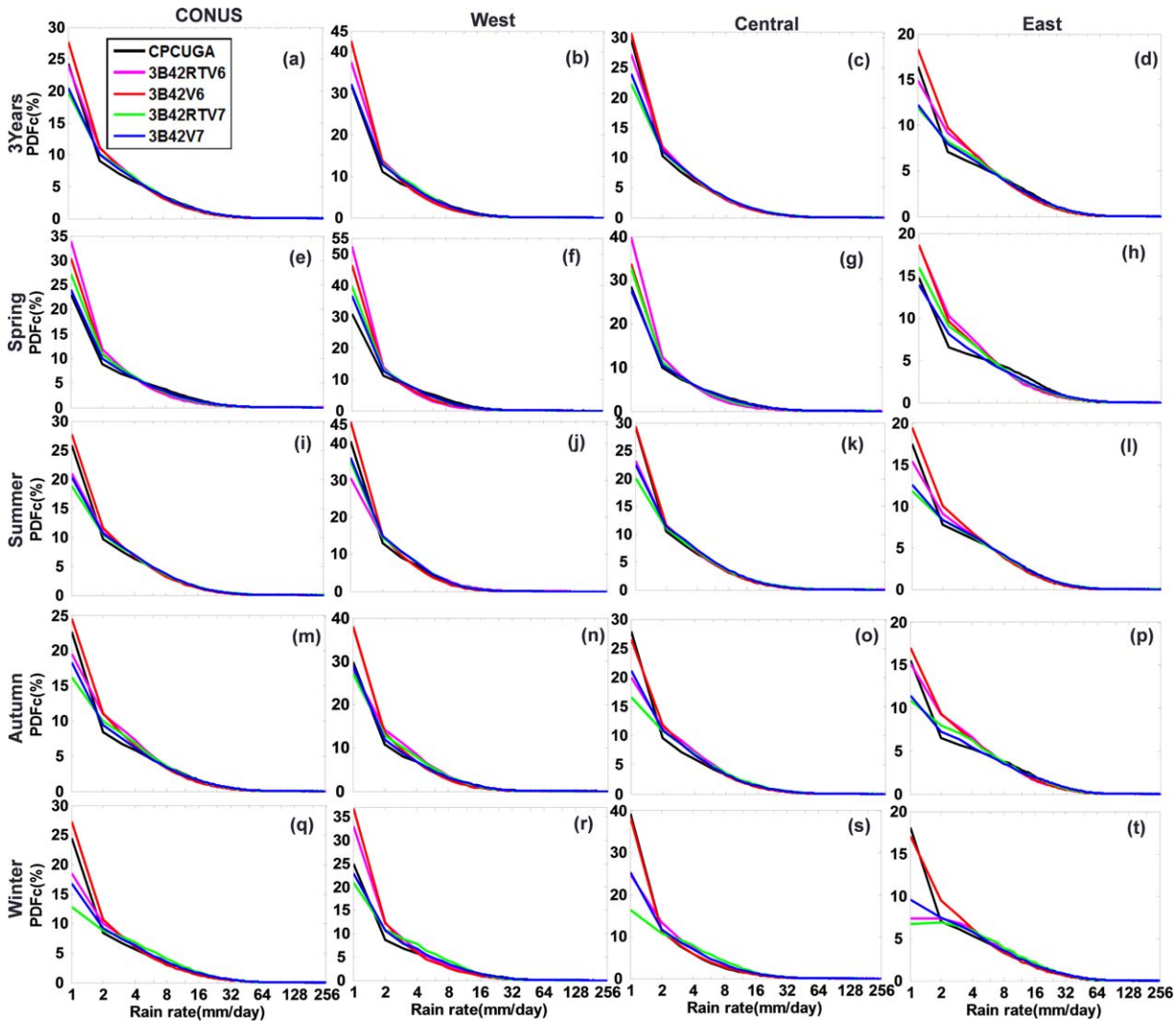

Figure 5. Probability distribution functions by occurrence (PDFc) with 1 mm/day interval and log space for *x* axis.

3.5. Contingency Statistics

[14] Figure 7 shows the performance of V6 and V7 TMPA products over the CONUS and three subregions in terms of probability of detection (POD), the critical successful index (CSI) and the false alarm rate (FAR) with thresholds from 1 to 250 mm/day with intervals of 1 mm/day. Scores of 3B42V6 and 3B42V7 are generally better than the real-time TMPA products CONUS-wide and for the three subregions. Specifically, 3B42V6 shows a little higher POD but much higher FAR than 3B42V7. Thus 3B42V7 has higher CSI skill scores than 3B42V6 over the CONUS and all subregions, particularly in the West. Compared to 3B42RTV6, 3B42RTV7 illustrates similar but a little better performance over the CONUS and three subregions. This implies that improvement of 3B42V7 over 3B42V6 is mainly a result of the gauge-correction procedure in the V7 TMPA algorithm by incorporating GPCC's "full" gauge analysis whenever available and the GPCC "monitoring" gauge analysis since 2010. In addition, it is worth noting that all products have low POD and CSI when rain rates are greater than 150 mm/day in the West. In the central and western regions, 3B42V7 and 3B42V6 demonstrate pronounced improvements in terms of CSI than their real-time counterparts when rain rates are greater than 50 mm/day. This means the real-time TMPA products underestimated the extremely heavy rainy events.

3.6. Spatial Distribution of Bias, RB, RMSE, and CC

[15] The distribution of the bias, RB, RMSE, and CC reveal the spatial performance of the TMPA data sets, which is important to hydrologic modelers for error propagation analysis in their simulations. Figure 8 shows the spatial distribution maps of bias, RB, RMSE, and CC versus the reference for annual precipitation. Figure 9 gives the corresponding PDFs by occurrence (PDFc) and cumulative distribution function by occurrence (CDFc) of the error statistics based on the data illustrated in Figure 8.

[16] Figure 8 shows that 3B42RTV6 and 3B42RTV7 overestimated precipitation in the north central CONUS, greatly underestimated along the west coast, and has low CCs (<0.5) in the intermountain West. The 3B42RTV7 shows improvements over 3B42RTV6 in the southeast

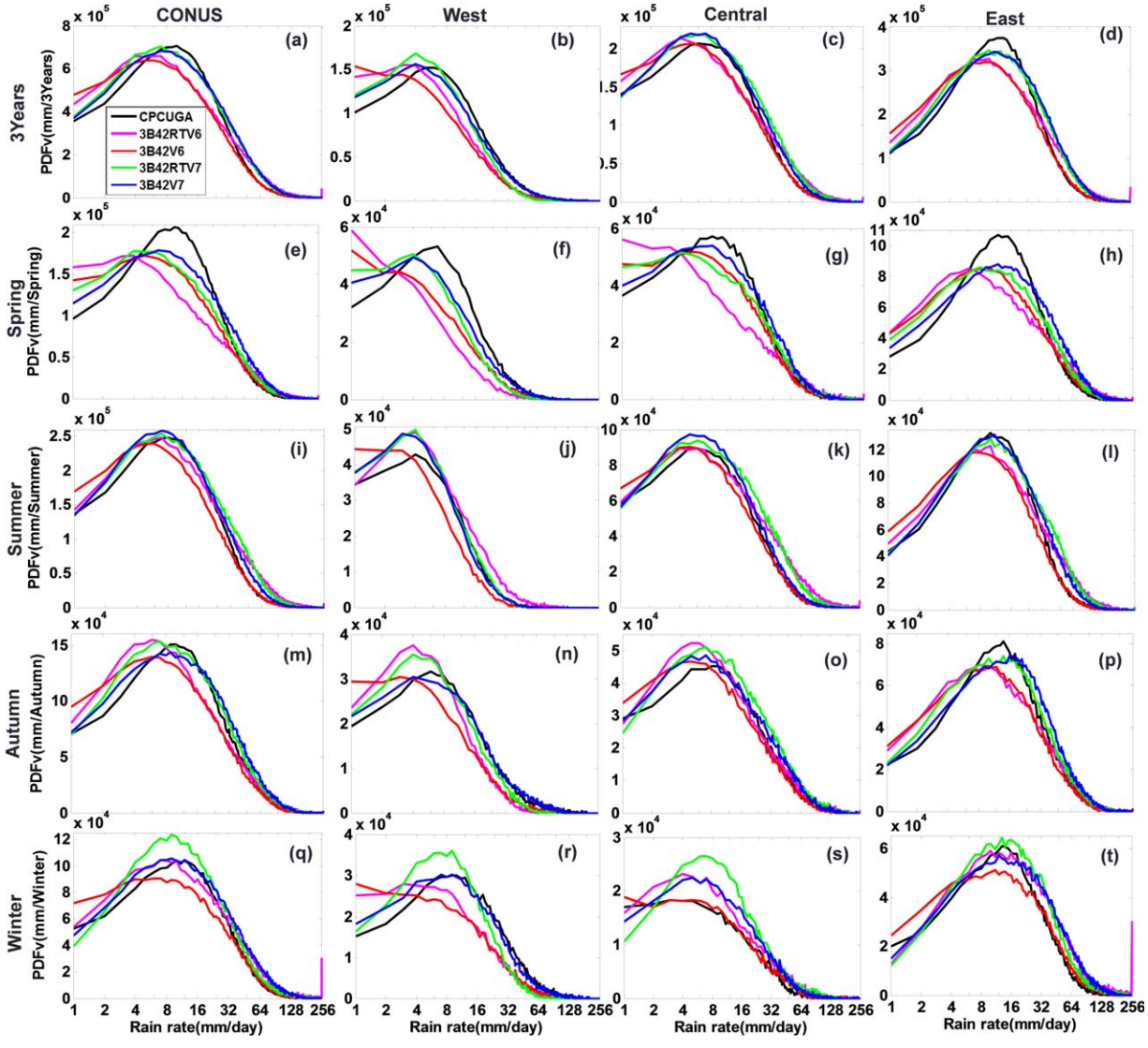

Figure 6. Probability distribution functions by volume (PDFv) with 1 mm/day interval and log space for *x* axis.

(i.e., Arkansas, Louisiana, Mississippi, Tennessee, Alabama, and Georgia) with less overestimation and lower RMSE. Product 3B42V6 has a dry bias compared to 3B42RTV6 in most of the central and eastern CONUS, which was evidently introduced through overcorrection in the gauge analysis (i.e., systematic underestimation) in Minnesota, Wisconsin, Illinois, Virginia, North Carolina, and Texas (see areas indicated by red letters A, B and C in Figure 1d. Moreover, the 3B42V6 shows similar underestimation of precipitation within the intermountain West with the other three products. Additionally, the 3B42V6 did not significantly improve the CC over the entire CONUS when compared to 3B42RTV6; whereas, the 3B42V7 not only shows better precipitation estimates in terms of bias but also improves CC over most areas in the CONUS. The 3B42V6 and 3B42V7 products have similar RMSE distributions over the western, central, and eastern CONUS and lower RMSE than real-time TMPA data sets (especially 3B42RTV6) in the southeast CONUS. All TMPA products have similar RMSE distributions in the western CONUS. This indicates that V7 TMPA data set did not significantly improve the RMSE in the West (see Figures 8k and 8o). Quantitatively, product 3B42V6 underestimated the precipitation by more than 10% in approximately 65.64% of the area, while 3B42V7 did so in about 29.70% of the area (Figure 8b). Looking at CC, PDFc, and CDFc, the 3B42V7 demonstrates much improvement over 3B42V6, which has a close CDFc and PDFc with 3B42RTV7. The CDFc with 3B42RTV6 shows distinct discrepancies with those of 3B42RTV7, 3B42RTV7 and 3B42V7. PDFc of 3B42RTV6 indicates it has fewer areas with a CC greater than 0.7, as compared to 3B42RTV7, 3B42V6, and 3B42V7. Generally, over the entire CONUS, all products have about 22.24% of the area with a high CC (>0.7), and relatively low CC distributions over the central and west mountainous regions, with 3B42RTV6, 3B42RTV7, 3B42RV6, and 3B42V7 each having 50.63%, 41.18%, 37.27%, and 30.55% of the area with a CC lower than 0.6, respectively.

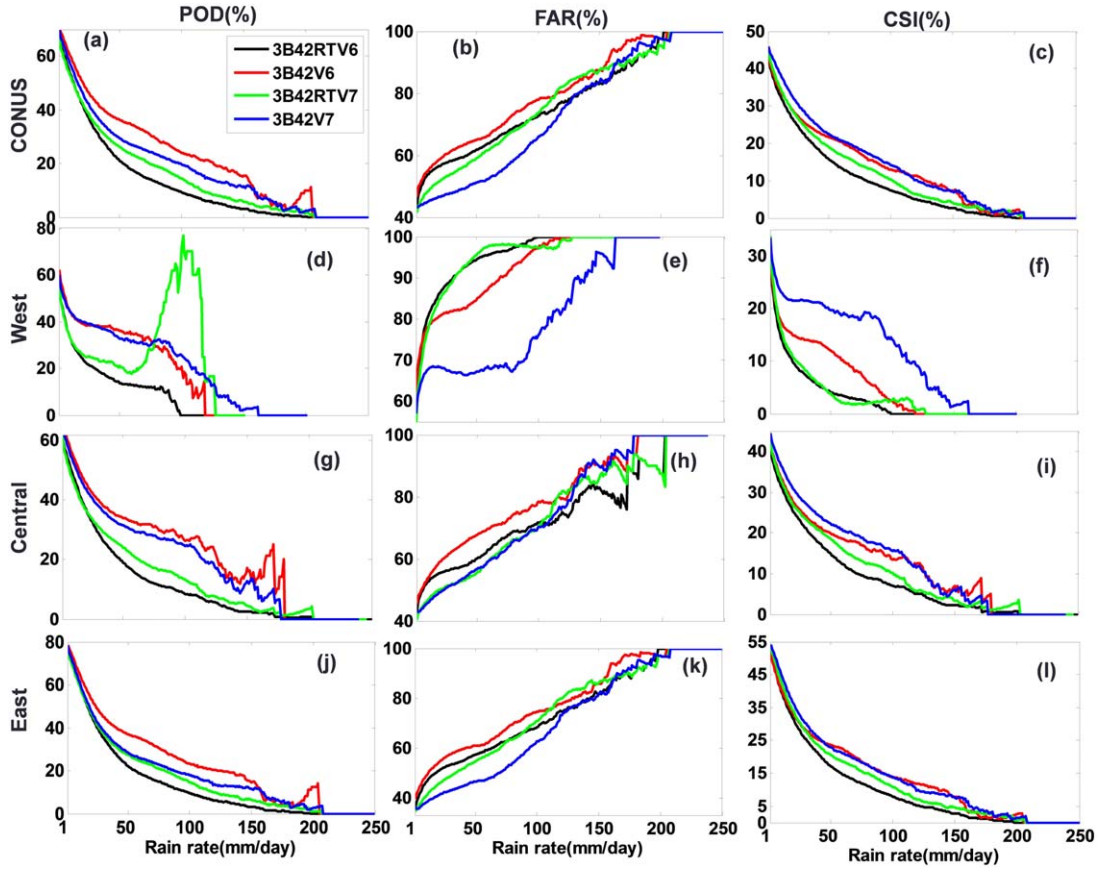

Figure 7. Contingency metrics of POD, FAR, and CSI over CONUS and three subregions West, Central, and East.

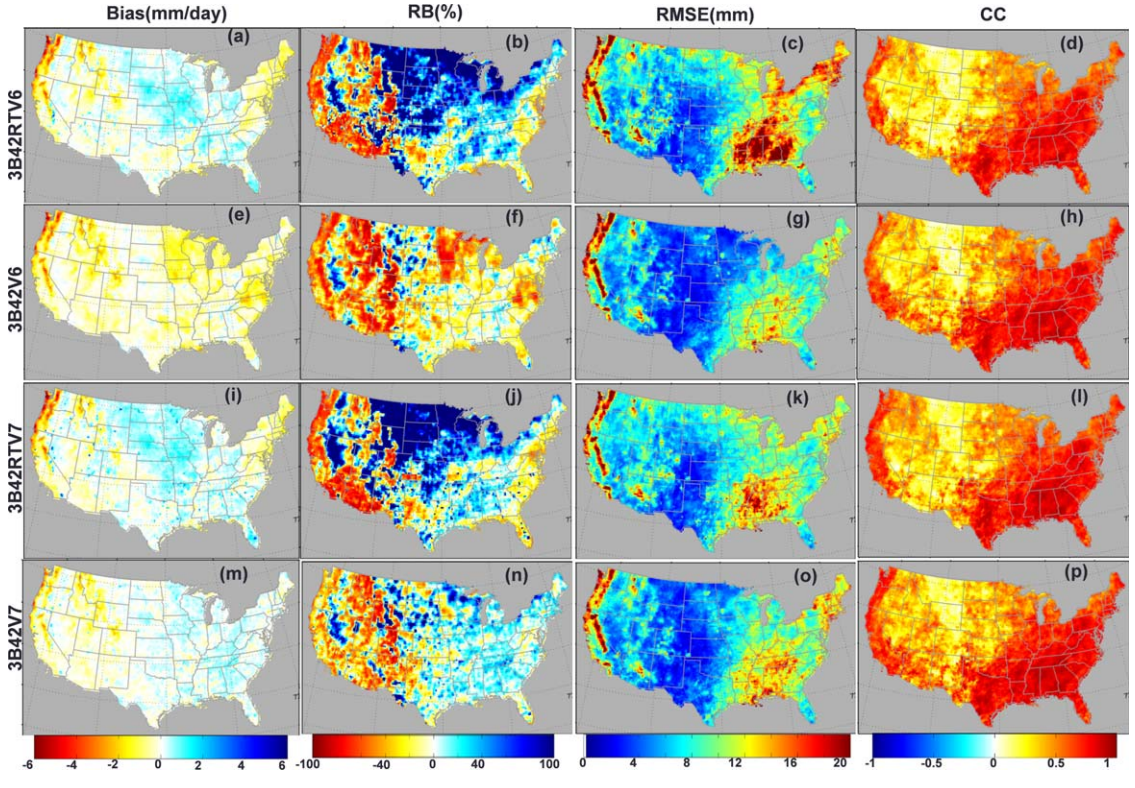

Figure 8. Spatial distributions of Bias, RB, RMSE, and CC.

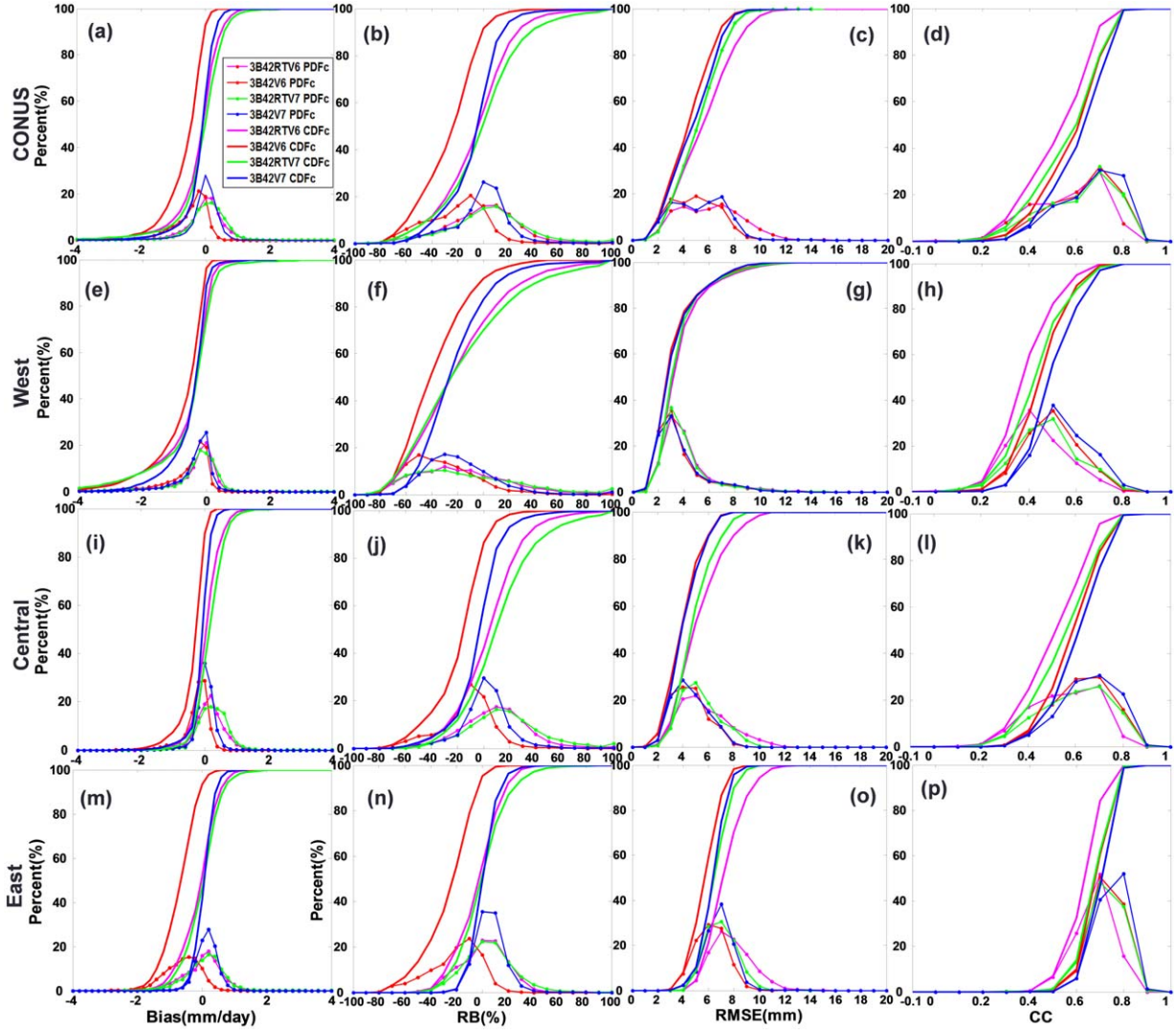

Figure 9. Probability (cumulative) distribution functions of Bias, RB, RMSE, and CC in Figure 8 by occurrence PDFc (CDFc).

4. Summary and Conclusions

[17] The TMPA products development team provides science communities with high-resolution global precipitation products based on merging passive microwave (PMW) and infrared (IR) satellite data with the new GPCC "full" gauge analysis, and the GPCC "monitoring" gauge analysis elsewhere when available. The latest V7 gauge-adjusted, post-real-time research product 3B42V7 represents an improvement over the previous V6 counterpart 3B42V6. This paper provides an early quantitative study of the spatial error characteristics of the real-time and post-processed version 6 and 7 TMPA products based on daily, seasonal, and interannual rainfall comparisons with the gauge-based CPCUGA product over a study period of three years over the CONUS. The findings of this study are summarized as follows:

[18] 1. The real-time products 3B42RTV6 and 3B42RTV7 overestimated precipitation by more than 20% for the three-year mean daily precipitation in the central and northern CONUS (i.e., east Montana, west North Dakota, South Dakota, Minnesota, Wisconsin, Iowa, and Illinois). The 3B42RTV7 saw improvement over 3B42RTV6 with less biased precipitation over the West, but it had more overestimation over the central and eastern CONUS.

[19] 2. Both 3B42RTV6 and 3B42V6 underestimated the three-year mean daily precipitation by more than 50% along the mountain ranges in the West, including the Cascades, Sierras, and the Rocky Mountains.

[20] 3. Seasonally, the 3B42V7 product distinctly outperformed the other three products from spring to winter with high CCs (0.84–0.96) and marginally biased precipitation (−8.03% to 3.11%) over the CONUS during every season. The 3B42V6 has lower CCs (0.77–0.90) and greater seasonally biased precipitation (−17.37% to −8.91%) over the CONUS. In the West, the 3B42V7 saw improvements with underestimation decreasing from −43.31% to −28.77% in spring, −25.66% to −5.80% in summer, −42.31% to −16.88% in autumn, and −52.83% to −36.21% in winter when compared to 3B42V6.

[21] 4. 3B42V6 has systematic gauge-adjustment issues (i.e., overcorrection) in Minnesota, Wisconsin, Illinois, Virginia, North Carolina, and Texas. These problems led to widespread rectangular-shaped regions of underestimation.

[22] 5. The 3B42V7 product improved significantly upon 3B42V6 in the West, where the bias was reduced greatly in 3B42V7. It corrected 3B42V6's over-adjustment problem in the central and northeast CONUS, and displayed spatially smooth and continuous variations of precipitation from the low to high precipitation areas. It improved the CC over the CONUS, especially in the West, and captured the CONUS-wide spatial patterns of 3 year mean daily precipitation with a high CC (0.92). Underestimation decreased from −22.95% to −2.37% and the RMSE decreased from 0.80 mm to 0.48 mm, compared to 3B42V6.

[23] 6. The 3B42V7 has higher comprehensive scores of CSI than 3B42V6 over the CONUS especially in the West. Compared to 3B42RTV6, the 3B42RTV7 illustrates close slightly better performance in the CONUS and the three subregions (Figure 7).

[24] 7. Both 3B42RTV6 and 3B42V6 generally saw more precipitation contributed by light precipitation rates (<6 mm/day) and less contribution by high precipitation rates (6–32 mm/day), while 3B42V7 has the overall best performance. This is most evident in the West.

[25] 8. The improvement of 3B42V7 over 3B42V6 is mainly from better incorporation of the GPCC data with improved climatology and anomaly analysis and resulting in significant improvements in complex terrain. It is noted, however, that the same climatological orographic enhancements are applied to the CPCUGA data used as reference in this study, thus the data sets are not independent. In the regions beyond the coverage (38°N-S) of TRMM, snow and ice covered surfaces likely cause the underestimation of TMPA products in the cold season, especially in the intermountain regions.

[26] The error characteristics of the TMPA's latest version products identified and quantified in this study will have significant implications for hydrological applications. The spatial error structure of TMPA products will provide hydrological modelers more insight into error sources when they conduct hydrological simulation in the western, central, and eastern CONUS during different seasons. The improvements reported for 3B42V7 over 3B42V6 have the ability to help the hydrological modelers retrospectively simulate surface runoff, while climate researchers can better understand the hydroclimate regime changes over the CONUS. This study shows quite clearly that the latest TMPA V7 product generally improves upon V6 over the CONUS, and additional studies around the world need to confirm if this generalization can apply elsewhere. Additional research is needed for QPE in the intermountain West regions, which is also problematic for ground-based radar measurements. Finally, more studies are needed to investigate the effect of the successive input SSMIS on the V7 TMPA. This study provides algorithm developers more confidence since the TMPA Version-7 is going to evolve as the Version-0 algorithm of the future GPM mission with anticipated launch date in 2014.

[27] **Acknowledgments.** This work was financially supported both by the NOAA Multi-function Phased-Array Radar Project administrated by the Advanced Radar Research Center at the University of Oklahoma and also by a NASA Global Precipitation Measurement Ground Validation program.

References

Bolvin, D. T., R. F. Adler, G. J. Huffman, E. J. Nelkin, and J. P. Poutiainen (2009), Comparison of GPCP monthly and daily precipitation estimates with high-latitude gauge observations, *J. Appl. Meteorol. Climatol.*, *48*(9), 1843–1857.

Chen, G., W. Sha, and T. Iwasaki (2009), Diurnal variation of precipitation over southeastern China: Spatial distribution and its seasonality, *J. Geophys. Res.*, *114*, D13103, doi:10.1029/2008JD011103.

Chen, M., P. Xie, and C. P. W. group (2008a), CPC unified gauge-based analysis of global daily precipitation, paper presented at 2008 Western Pacific Geophysics Meeting, AGU, Cairns, Australia.

Chen, M., W. Shi, P. Xie, V. B. S. Silva, V. E. Kousky, R. W. Higgins, and J. E. Janowiak (2008b), Assessing objective techniques for gauge-based analyses of global daily precipitation, *J. Geophys. Res.*, *113*, D04110, doi:10.1029/2007JD009132.

Chen, S., J. J. Gourley, Y. Hong, P. E. Kirstetter, J. Zhang, K. Howard, Z. L. Flamig, J. Hu, and Y. Qi (2013), Evaluation and uncertainty estimation of NOAA/NSSL next generation National Mosaic QPE (Q2) over the Continental United States, *J. Hydrometeorol.*, *14*, 1308–1322.

Chen, S., Y. Hong, Q. Cao, P. E. Kirstetter, J. J. Gourley, Y. Qi, J. Zhang, K. Howard, J. Hu, and J. Wang (2012b), Performance evaluation of radar and satellite rainfalls for typhoon morakot over Taiwan: Are remote-sensing products ready for gauge denial scenario of extreme events?, *J. Hydrol.*, doi:10.1016/j.jhydrol.2012.12.026.

Chen, S., P. E. Kirstette, Y. Hong, J. Gourley, J. Zhang, K. Howard, and J. Hu (2012a), Quantification of spatial errors of precipitation rates and types from the TRMM precipitation radar (the latest successive V6 and V7) over the United States, paper presented at 2012 Fall Meeting, AGU, San Francisco, Calif., 3–7 Dec.

Daly, C., R. P. Neilson, and D. L. Phillips (1994), A statistical-topographic model for mapping climatological precipitation over mountainous terrain, *J. Appl. Meteorol.*, *33*(2), 140–158.

Ferraro, R. R., E. A. Smith, W. Berg, and G. J. Huffman (1998), A screening methodology for passive microwave precipitation retrieval algorithms, *J. Atmos. Sci.*, *55*(9), 1583–1600.

Gourley, J. J., Y. Hong, Z. L. Flamig, L. Li, and J. Wang (2010), Intercomparison of rainfall estimates from radar, satellite, gauge, and combinations for a season of record rainfall, *J. Appl. Meteorol. Climatol.*, *49*(3), 437–452.

Grody, N. C. (1991), Classification of snow cover and precipitation using the special sensor microwave imager, *J. Geophys. Res.*, *96*, 7423–7435.

Hirpa, F. A., M. Gebremichael, and T. Hopson (2010), Evaluation of high-resolution satellite precipitation products over very complex terrain in Ethiopia, *J. Appl. Meteorol. Climatol.*, *49*(5), 1044–1051.

Hong, Y., and R. Adler (2007), Towards an early-warning system for global landslides triggered by rainfall and earthquake, *Int. J. Remote Sens.*, *28*(16), 3713–3719.

Hong, Y., K. Hsu, H. Moradkhani, and S. Sorooshian (2006), Uncertainty quantification of satellite precipitation estimation and Monte Carlo assessment of the error propagation into hydrologic response, *Water Resour. Res.*, *42*, W08421, doi:10.1029/2005WR004398.

Huffman, G. J., and D. T. Bolvin (2013), *TRMM and Other Data Precipitation Data Set Documentation*, Lab. for Atmos., NASA Goddard Space Flight Cent. and Sci. Syst. and Appl. [Available at: http://precip.gsfc.nasa.gov/pub/trmmdocs/3B42_3B43_doc.pdf.]

Huffman, G. J., R. F. Adler, D. T. Bolvin, and E. J. Nelkin (2010), The TRMM Multi-satellite Precipitation Analysis (TMPA), in *Satellite Rainfall Applications for Surface Hydrology*, edited by F. Hossain and M. Gebremichael, pp. 3–22, Springer, New York.

Huffman, G. J., D. T. Bolvin, E. J. Nelkin, D. B. Wolff, R. F. Adler, G. Gu, Y. Hong, K. P. Bowman, and E. F. Stocker (2007), The TRMM multisatellite precipitation analysis (TMPA): Quasi-global, multiyear, combined-sensor precipitation estimates at fine scales, *J. Hydrometeorol.*, *8*(1), 38–55.

Huffman, G. J., D. T. Bolvin, E. J. Nelkin, and R. F. Adler (2011), Highlights of version 7 TRMM multisatellite precipitation analysis (TMPA), paper presented at the 5th International. Precipitation Working Group Workshop, Workshop Program and Proceedings, 11–15 Oct., Hamburg, Germany, edited by C. Klepp and G. Huffman, Reports on Earth Syst. Sci., 100/2011, Max-Planck-Institut für Meteorologie, pp. 109–110.

Kirstetter, P.-E., Y. Hong, J. Gourley, M. Schwaller, W. Petersen, and J. Zhang (2013), Comparison of TRMM 2A25 products version 6 and Version 7 with NOAA/NSSL ground radar-based national mosaic QPE, *J. Hydrometeorol.*, *14*(2), 661–669.

Liang, X., E. F. Wood, and D. P. Lettenmaier (1996), Surface soil moisture parameterization of the VIC-2L model: Evaluation and modification, *Global Planet. Change*, *13*(1), 195–206.

Liang, X., D. P. Lettenmaier, E. Wood, and S. Burges (1994), A simple hydrologically based model of land surface water and energy fluxes for general circu-lation models, *J. Geophys. Res*, *99*, 14,415–14,428.

Negri, A. J., and R. F. Adler (1993), An intercomparison of three satellite infrared rainfall techniques over Japan and surrounding waters, *J. Appl. Meteorol.*, *32*(2), 357–373.

Shen, Y., A. Xiong, Y. Wang, and P. Xie (2010), Performance of high-resolution satellite precipitation products over China, *J. Geophys. Res.*, *115*, D02114, doi:10.1029/2009JD012097.

Stampoulis, D., and E. N. Anagnostou (2012), Evaluation of global satellite rainfall products over continental Europe, *J. Hydrometeorol.*, *13*(2), 588–603.

Stephens, G. L., and C. D. Kummerow (2007), The remote sensing of clouds and precipitation from space: A review, *J. Atmos. Sci.*, *64*(11), 3742–3765.

Su, F., Y. Hong, and D. P. Lettenmaier (2008), Evaluation of TRMM multisatellite precipitation analysis (TMPA) and its utility in hydrologic prediction in the La Plata Basin, *J. Hydrometeorol.*, *9*(4), 622–640.

Tian, Y., C. D. Peters-Lidard, B. J. Choudhury, and M. Garcia (2007), Multitemporal analysis of TRMM-based satellite precipitation products for land data assimilation applications, *J. Hydrometeorol.*, *8*(6), 1165–1183.

Tian, Y., C. D. Peters-Lidard, R. F. Adler, T. Kubota, and T. Ushio (2010), Evaluation of GSMaP precipitation estimates over the contiguous United States, *J. Hydrometeorol.*, *11*(2), 566–574.

Tuttle, J. D., R. E. Carbone, and P. A. Arkin (2008), Comparison of ground-based radar and geosynchronous satellite climatologies of warm-season precipitation over the United States, *J. Appl. Meteorol. Climatol.*, *47*(12), 3264–3270.

Vicente, G. A., R. A. Scofield, and W. P. Menzel (1998), The operational GOES infrared rainfall estimation technique, *Bull. Am. Meteorol. Soc.*, *79*(9), 1883–1898.

Vila, D., R. Ferraro, and R. Joyce (2007), Evaluation and improvement of AMSU precipitation retrievals, *J. Geophys. Res.*, *112*, D20119, doi: 10.1029/2007JD008617.

Wu, H., R. F. Adler, Y. Hong, Y. Tian, and F. Policelli (2012), Evaluation of global flood detection using satellite-based rainfall and a hydrologic model, *J. Hydrometeorol.*, *13*, 1268–1284, doi:10.1175/jhm-d-11-087.1.

Yong, B., L. L. Ren, Y. Hong, J. H. Wang, J. J. Gourley, S. H. Jiang, X. Chen, and W. Wang (2010), Hydrologic evaluation of multisatellite precipitation analysis standard precipitation products in basins beyond its inclined latitude band: A case study in Laohahe basin, China, *Water Resour. Res*, *46*, W07542, doi:10.1029/2009WR008965.

Yong, B., Y. Hong, L. L. Ren, J. J. Gourley, G. J. Huffman, X. Chen, W. Wang, and S. I. Khan (2012), Assessment of evolving TRMM-based multisatellite real-time precipitation estimation methods and their impacts on hydrologic prediction in a high latitude basin, *J. Geophys. Res.*, *117*, D09108, doi:10.1029/2011JD017069.

Zhou, T., R. Yu, H. Chen, A. Dai, and Y. Pan (2008), Summer precipitation frequency, intensity, and diurnal cycle over China: A comparison of satellite data with rain gauge observations, *J. Clim.*, *21*(16), 3997–4010.